Iranian Journal of Pharmaceutical Sciences
2026: 22 (1): 466-475
https://journals.sbmu.ac.ir/IJPS

Research Article

OPEN ACCESS

Elderberry-Derived Anthocyanins as Multitarget Inhibitors of Influenza a Viral Proteins: Molecular Docking and ADMET Analysis

Samiran Sadhukhan[a], Subarna Ganguli[b]*

[a] *Department of Pharmaceutical Chemistry, Netaji Subhas Chandra Bose Institute of Pharmacy, Chakdah, WB, India.*
[b] *Department of Pharmaceutical Chemistry, Radiant Institute of Pharmaceutical Sciences, Salki, Tengarmari, Kishanganj, Bihar-855107,India.*

Received: October 17, 2025 **Accepted:** October 10, 2026 **Available online:** November 7, 2026.

Abstract

Influenza A virus continues to evolve and has shown a steady rise in resistance to commonly used antiviral drugs, which reinforces the need for new therapeutic candidates. In this work, anthocyanin glycosides from elderberry (*Sambucus nigra*) were examined for their ability to interact with three key influenza A proteins. Five major moleculescyanidin-3-glucoside, delphinidin-3-glucoside, pelargonidin-3-glucoside, malvidin-3-glucoside, and petunidin-3-glucoside- were docked using AutoDock Vina against neuraminidase (4MWW), hemagglutinin (4BSD), and PA endonuclease (6FS7), and native ligands were redocked to verify docking reliability. Cyanidin-3-glucoside showed the best affinity towards neuraminidase, even stronger than the reference ligand, while delphinidin-3-glucoside and pelargonidin-3-glucoside displayed strong binding at the PA endonuclease site. Hemagglutinin binding was comparatively moderate across all compounds.ADMET predictions suggested favorable pharmacokinetic characteristics, including no predicted hepatotoxicity or skin sensitization, although several compounds showed limited oral absorption. Overall, these computational findings suggest that elderberry anthocyanins may interact with multiple influenza A viral proteins and warrant further experimental investigation through biochemical and cellular assays to validate their antiviral potential.

Keywords: Influenza A; Neuraminidase; PA endonuclease; Anthocyanins; Elderberry; Molecular docking.

1. Introduction

Influenza A remains a persistent global health concern due to its ability to cause recurrent seasonal outbreaks, severe respiratory illness, and pandemic-scale mortality [1]. The virus continues to evolve, and the rapid emergence of drug-resistant strains has begun to undermine the effectiveness of existing antiviral therapies. Polymerase inhibitors such as baloxavir and neuraminidase inhibitors such as oseltamivir are widely used; however, several circulating influenza variants have already shown reduced susceptibility [2, 3]. This highlights the need to discover new therapeutic agents capable of acting on multiple viral targets and interrupting different stages of the viral life cycle.

Natural polyphenols, derived from plant sources, have received increasing attention as potential antiviral

*** Corresponding Author**:
Subarna Ganguli, Department of Pharmaceutical Chemistry, Radiant Institute of Pharmaceutical Sciences, Salki, Tengarmari, Kishanganj, Bihar-855107,India. E-mail: samiranrana05@gmail.com.

Cite this article as: Sadhukhan S., Ganguli S. Elderberry-Derived Anthocyanins as Multitarget Inhibitors of Influenza a Viral Proteins: Molecular Docking and ADMET Analysis. Iran. J. Pharm. Sci., 2026, 22 (1): 466- 475.

DOI: https://doi.org/10.22037/ijps.v22i1.50670

This open-access article is distributed under the terms of the Creative Commons Attribution Non Commercial 4.0 License (CC BY-NC 4.0).

compounds due to their structural diversity, broad biological activity, and relatively low toxicity profiles [4]. Among these molecules, anthocyanin glycosides are the primary bioactive constituents of *Sambucus nigra* (elderberry), a medicinal plant traditionally used for immune support and respiratory infections [5]. Previous experimental and clinical observations suggest that elderberry-derived anthocyanins possess antiviral potential, although their molecular-level interactions with influenza a proteins remain insufficiently explored.

The present study employs molecular docking, drug-likeness profiling, and ADMET (absorption, distribution, metabolism, excretion, and toxicity) evaluation to investigate the inhibitory potential of five major elderberry anthocyanins against neuraminidase, hemagglutinin, and PA endonuclease- three critical proteins involved in influenza A replication and host infection. This work aims to provide an initial foundation for identifying natural molecular scaffolds that can interfere with viral function and to compare their binding characteristics with reference antiviral agents. The findings provide preliminary computational evidence that may support future experimental investigations into elderberry-derived anthocyanins as potential anti-influenza lead compounds.

2. Materials and methods

2.1. Molecular docking

We collected five anthocyanin glycosides from the PubChem database in 3D SDF format. These ligands were loaded into PyRx (v0.8) and subjected to energy minimization with the Universal Force Field (UFF). We applied the conjugate-gradient method for 1000 iterations, with a convergence limit of 0.1 kcal/mol, to obtain the lowest-energy conformations. After optimization, we saved each structure in PDBQT format [6, 7]. Crystal structures of the target proteins were downloaded from the RCSB Protein Data Bank and prepared using Discovery Studio 2024. We used the native ligands as reference controls to locate and validate the active binding pocket. Grid boxes were then positioned around the native ligand region to ensure that docking took place within the functional site of each protein.

Molecular docking was carried out in AutoDock Vina through the PyRx interface [8, 9], and an exhaustiveness value of 20 was used for all runs. Binding affinity values (kcal/mol) served as the main selection criteria to compare how strongly each ligand interacted with the receptors. Discovery Studio was used for 2D interaction mapping, while PyMOL (v2.3) was used to visualize 3D binding poses [10].

2.2. Docking validation

We removed the co-crystallized ligands from each protein structure and reinserted them into the active sites to ensure the docking procedure was correct. After removing all non-protein atoms from the crystal structure, the ligand was exported in PDB format in order to obtain the ligand coordinates.

To maintain consistency, we re-docked the compounds using identical grid configurations and docking parameters. After docking, we used PyMOL to overlay each native ligand's projected binding pose with its initial crystallographic orientation. This is followed by the determination of the root-mean-square deviation (RMSD). An RMSD value within the permitted range indicates that the docking method can replicate the experimental binding configuration. Ligand-protein interactions were additionally evaluated using LigPlot+ (v2.2.8) to confirm and compare the persistence of key binding contacts [11].

2.3. Screening for Drug Likeness and ADMET

The SwissADME and pkCSM online servers were used to investigate the pharmacokinetics and drug-likeness of the anthocyanin glycosides. SwissADME was used to determine MW, LogP, and the number of hydrogen-bond donors and acceptors. Lipinski's Rule of Five was used to assess the drug-like qualities of each compound [12]. The SMILES structure was provided for each compound, and pkCSM was used to predict ADMET properties. The following parameters were also taken into consideration, such as absorption (water solubility), distribution (volume of distribution, intestinal and skin permeability, Caco-2 permeability), excretion (total clearance, renal OCT2 affinity), metabolism (CYP450 enzyme interactions), and toxicity (hepatotoxicity, skin sensitization, and maximum tolerated dose). Forecasts using default parameters and their results helped select the main candidates for further experimental validation [13].

This open-access article is distributed under the terms of the Creative Commons Attribution Non Commercial 4.0 License (CC BY-NC 4.0).

3. Result and discussion

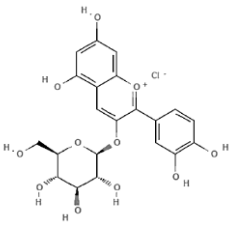
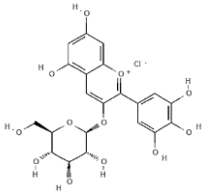
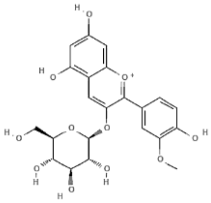
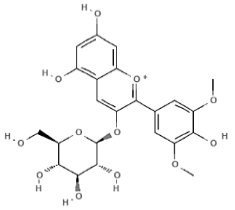
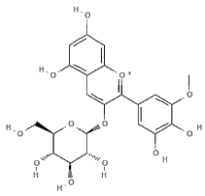
3.1. Selection of Ligands and Protein Targets

This study examined five anthocyanin glycosides from elderberries, namely petunidin-3-glucoside (Pt3G), peonidin-3-glucoside (P3G), malvidin-3-glucoside (M3G), cyanidin-3-glucoside (C3G), and delphinidin-3-glucoside (D3G). We evaluated these compounds for their inhibitory potential against three key influenza A proteins: neuraminidase (NA; PDB ID: 4MWW), hemagglutinin (HA; PDB ID: 4BSD), and PA endonuclease (PA; PDB ID: 6FS7). Each target contributes to a distinct stage of the viral life cycle: neuraminidase mediates viral release, hemagglutinin enables host-cell entry, and PA endonuclease supports genome replication. The high-quality crystallographic structures of these proteins, resolved at 1.90-2.40 Å, are summarized in **Table 1**. The chemical structures and physicochemical characteristics of the selected anthocyanins are provided in **Table 2**.

Table 1. Selected Influenza a virus targets with PDB ID, method, and resolution.

Sl No	Protein	PDB ID	Organism	Method	Resolution	Reference
1	Neuraminidase (NA)	4MWW	Influenza A virus	X-ray diffraction	1.90 Å	[14]
2	Hemagglutinin (HA)	4BSD	Influenza A virus	X-ray diffraction	2.40 Å	[15]
3	PA endonuclease (PA)	6FS7	Influenza A virus	X-ray diffraction	1.96 Å	[16]

Table 2. Selected phytochemicals with their PubChem ID and 2D structures.

Sl No	Compounds	PubChem ID	Formula	Structure
1	Cyanidin-3-glucoside (C3G)	197081	$C_{21}H_{21}ClO_{11}$	
2	Delphinidin-3-glucoside (D3G)	165558	$C_{21}H_{21}ClO_{12}$	
3	Peonidin-3-glucoside (P3G)	443654	$C_{22}H_{23}O_{11}^{+}$	
4	Malvidin-3-glucoside (M3G)	443652	$C_{23}H_{25}O_{12}^{+}$	
5	Petunidin-3-glucoside (Pt3G)	443651	$C_{22}H_{23}O_{12}^{+}$	

This open-access article is distributed under the terms of the Creative Commons Attribution Non Commercial 4.0 License (CC BY-NC 4.0).

3.2. Docking Results and Binding Affinity Evaluation

Docking outcomes revealed clear differences in the binding performance of the five anthocyanins across the three influenza a targets (**Table 3**). Among them, cyanidin-3-glucoside (C3G) demonstrated the most favorable affinity toward neuraminidase (–8.9 kcal/mol), outperforming the reference inhibitor oseltamivir (–6.7 kcal/mol). This suggests a more stable interaction within the neuraminidase catalytic pocket and indicates that C3G may possess superior inhibitory potential compared to the clinically established drug.

Binding to hemagglutinin was comparatively weaker, with docking energies ranging from –6.4 to –6.8 kcal/mol, values closely aligned with the sialic acid analog (–6.6 kcal/mol). These results suggest that while anthocyanins can engage the hemagglutinin binding site, they likely act as moderate competitive ligands rather than strong blockers of viral entry. The most prominent interaction trend was observed at the PA endonuclease domain. Delphinidin-3-glucoside (D3G) and peonidin-3-glucoside (P3G) reached docking scores of –8.3 kcal/mol, approaching the affinity of baloxavir acid (–9.7 kcal/mol), the approved PA inhibitor. This suggests these compounds may interfere with endonuclease-mediated RNA processing, a critical step in viral transcription. Malvidin-3-glucoside (M3G) and petunidin-3-glucoside (Pt3G) also showed favorable binding, though with slightly weaker affinities (–7.9 to –8.2 kcal/mol), suggesting that all five ligands are compatible with replication-associated catalytic residues.

Overall, the comparative docking profile identifies C3G as the strongest neuraminidase binder, whereas D3G and P3G emerge as promising PA endonuclease inhibitors. These observations suggest potential multi-target binding behavior, which may be useful for further experimental evaluation. **Table 4** provides the docking grid coordinates for all proteins to confirm that ligand placement was restricted to validated, biologically relevant binding regions.

3.3. Validation of Docking Protocol

We assessed the reliability of the docking workflow by re-docking the native ligands into their corresponding protein active sites. Superimposition of the crystallographic and re-docked poses resulted in RMSD values of 2.203 Å for neuraminidase (4MWW), 2.901 Å for hemagglutinin (4BSD), and 2.230 Å for PA endonuclease (6FS7), all falling within the generally accepted limit of <3.0 Å (**Figure 1**) [17]. These values indicate that the docking settings were able to reproduce the experimental binding orientation with good structural agreement.

LigPlot+ analysis further supported this by showing that re-docked ligands preserved the characteristic interaction networks observed in the native structures, including hydrogen bonds and hydrophobic contacts at the catalytic sites of neuraminidase, hemagglutinin, and PA endonuclease (**Figure 2**). The consistency of these contacts across all three proteins suggests that the protocol maintained both conformation and residue-level recognition. Taken together, the RMSD and interaction patterns confirm that the docking protocol is reliable, and the predicted anthocyanin binding can be interpreted with confidence.

Table 3. Binding energies (in kcal/mol) of selected phytochemicals and native standards against target receptor proteins.

PDB ID	C3G	D3G	P3G	M3G	Pt3G	Native-ligand
4MWW	-8.9	-8.8	-8.7	-8.5	-8.7	-6.7 (Oseltamivir)
4BSD	-6.8	-6.4	-6.8	-6.6	-6.4	-6.6 (Sialic acid analog)
6FS7	-8.2	-8.3	-8.3	-7.9	-8.2	-9.7 (Baloxavir acid)

Table 4. AutoDock Vina grid box parameters for molecular docking.

PDB ID	Vina Search Space					
	Ceter			Dimensions (Å)		
	X	Y	Z	X	Y	Z
4MWW	-17.49	26.71	61.75	25	25	25
4BSD	34.08	-32.85	34.22	25	25	25
6FS7	-38.43	5.73	-36.83	25	25	25

This open-access article is distributed under the terms of the Creative Commons Attribution Non Commercial 4.0 License (CC BY-NC 4.0).

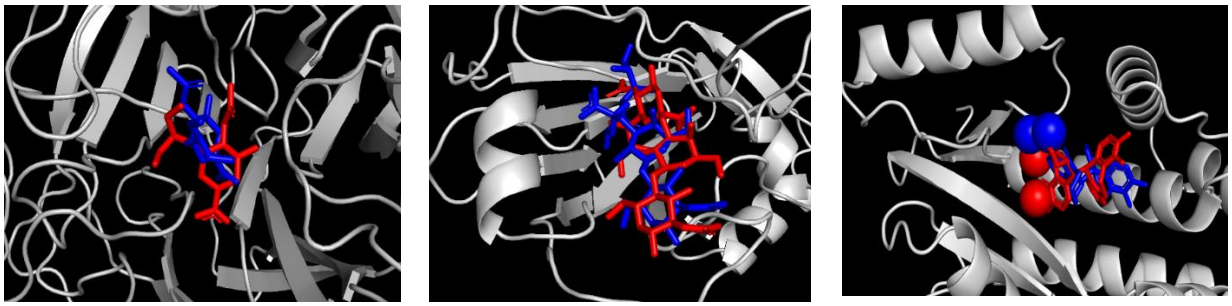


Figure 1. Superimposition of re-docked (blue) and native (red) ligands in proteins 4MWW (a), 4BSD(b), and 6FS7 (c) active sites (RMSD = 2.203Å, 2.901 Å, and 2.23 Å, respectively)

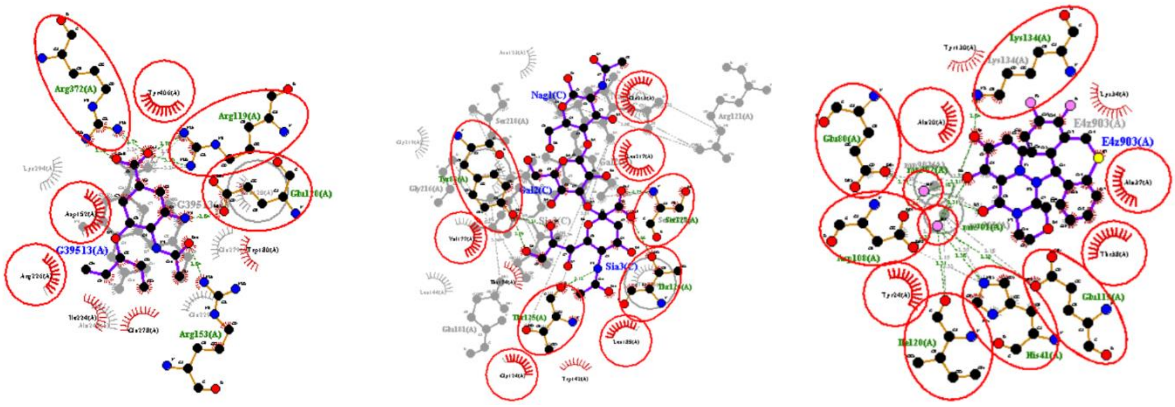


Figure 2. LigPlot+ interactions of re-docked ligands in 4MWW, 4BSD, and 6FS8, with overlapping residues to native ligands marked in red.

3.4. Visualization and Interaction Analysis

Molecular interaction analyses were conducted to investigate how anthocyanin glycosides bind within the active sites of neuraminidase, hemagglutinin, and PA endonuclease. **Table 5** summarizes the interaction profiles, and **Figure 3** illustrates them, with direct comparisons to the native inhibitors.

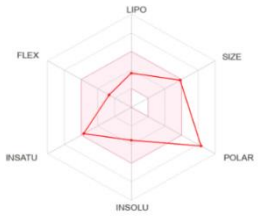
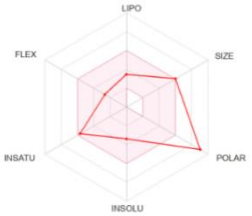
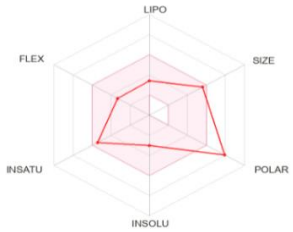
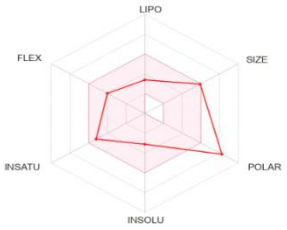
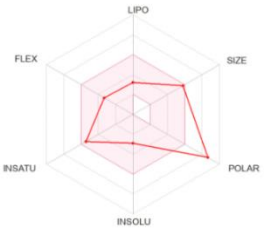
In the neuraminidase (4MWW) complexes, C3G interacted with GLY349, ASN348, and GLU279, while stabilizing through hydrophobic contacts with ILE224 and ALA248. D3G displayed a similar pattern, engaging ARG372, ASN296, and TYR406 in addition to residues shared with C3G. By contrast, the native ligand oseltamivir established multiple polar contacts, including LYS294, ARG119, ARG372, and ARG226, as well as hydrophobic interactions involving ILE224 and GLU278. The overlap of anthocyanin interactions with oseltamivir's binding pocket suggests that C3G and D3G may act as competitive inhibitors (**Figure 4**).

For hemagglutinin (4BSD), C3G formed hydrogen bonds with ARG121 and VAL177, complemented by hydrophobic interactions with LEU144 and TRP142. P3G engaged SER134 alongside the same hydrophobic residues, indicating a similar binding orientation. The native sialic acid analog, however, displayed a broader interaction profile, contacting residues such as GLY216, GLY219, SER218, ARG121, GLU81, and THR125, with additional stabilization from HIS174. This more extensive binding network highlights the natural ligand's stronger complementarity to the hemagglutinin pocket, whereas anthocyanins appear to mimic its interactions partially.

In the PA endonuclease (6FS7) complexes, D3G engaged catalytic residues GLU119 and ILE120 along with ARG82 and TYR24, while P3G formed interactions with GLU119, LYS134, and PRO107. Both anthocyanins also stabilized binding through hydrophobic contacts with TYR24, HIS41, and THR38, residues critical for the enzymatic function of the endonuclease domain. The native ligand baloxavir acid displayed a complementary binding pattern, with strong interactions involving LYS34 and LYS134 and hydrophobic contributions from TYR24, ALA37, THR38, and HIS41. The shared engagement of these catalytic residues indicates that anthocyanins may interfere with the same functional site as baloxavir, albeit with slightly weaker affinity.

This open-access article is distributed under the terms of the Creative Commons Attribution Non Commercial 4.0 License (CC BY-NC 4.0).

Table 5. Drug-likeness and Radar plot of selected glycosides based on Lipinski's rule using SwissADME.

Compounds	MW (gm/mol)	NHA	NHD	Logp (clogp)	Lipinski's rule violation	Radar Plot
C3G	484.84	11	8	-2.17	2	
D3G	500.84	12	9	-2.63	3	
P3G	463.42	11	7	-0.69	2	
M3G	493.44	12	7	-1.29	2	
Pt3G	479.41	12	8	-0.90	2	

This open-access article is distributed under the terms of the Creative Commons Attribution Non Commercial 4.0 License (CC BY-NC 4.0).

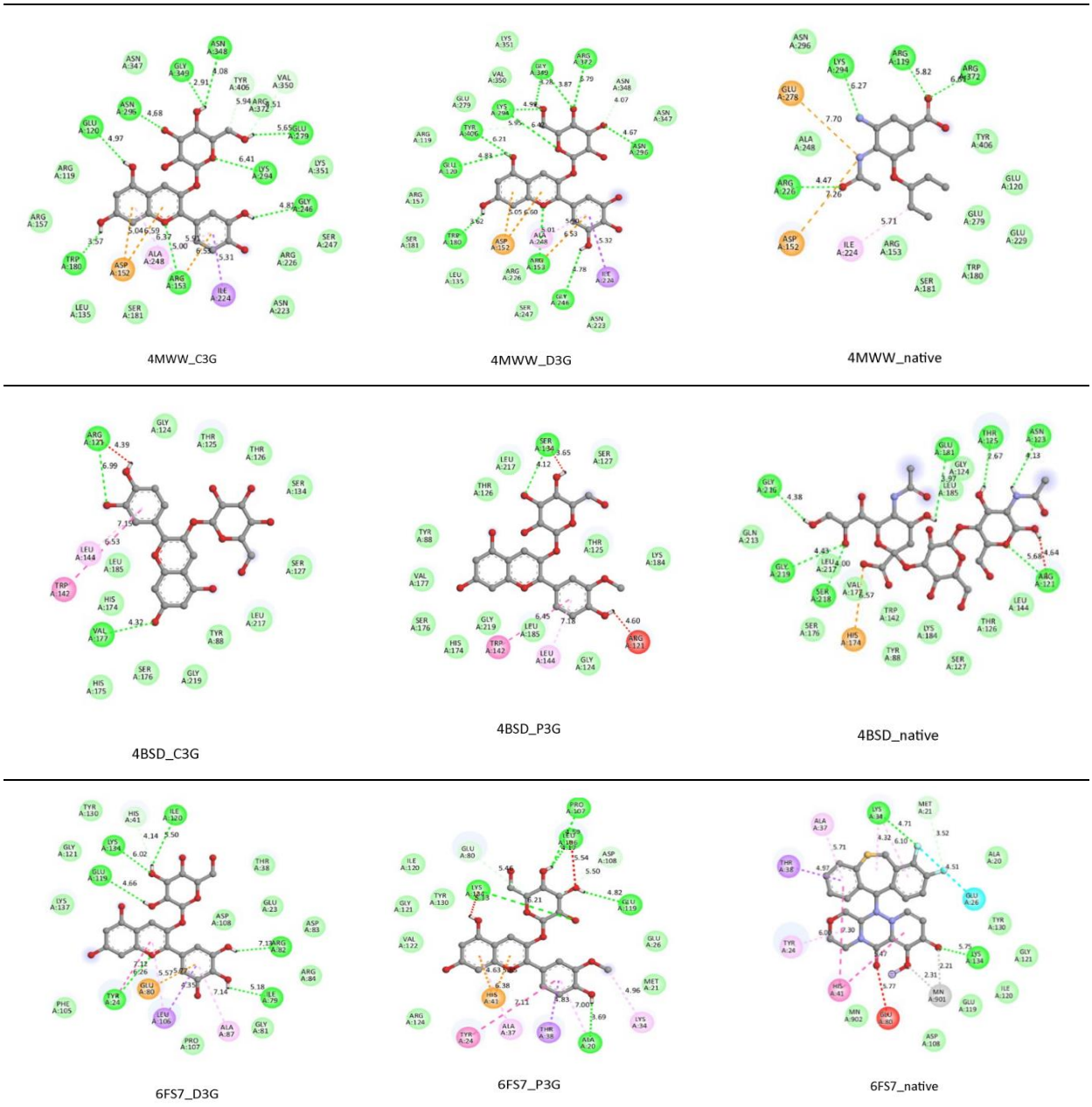


Figure 3. 2D interaction profiles of top-ranked ligands and native inhibitors with 4MWW, 4BSD, and 6FS7

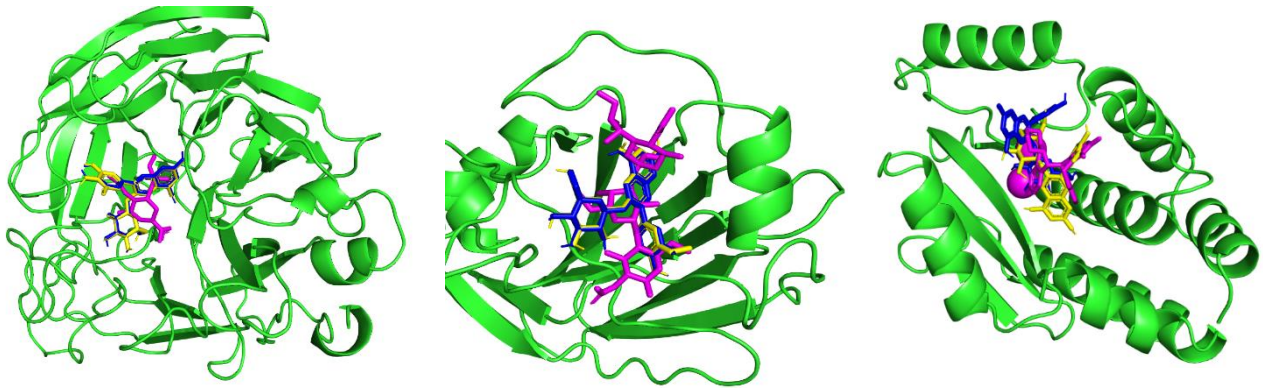


Figure 4. Binding site comparison for neuraminidase (4MWW), hemagglutinin (4BSD), and PA endonuclease (6FS7), showing superimposed docking poses of native ligands (magenta) and anthocyanins (blue and yellow).

This open-access article is distributed under the terms of the Creative Commons Attribution Non Commercial 4.0 License (CC BY-NC 4.0).

These results indicate that the binding behavior of anthocyanin glycosides aligns with that of the native inhibitors in several respects. In neuraminidase, C3G showed an interaction profile that closely resembled oseltamivir, suggesting that it could interfere with viral release similarly. For PA endonuclease, D3G and P3G shared key residue contacts with baloxavir acid, suggesting they may also affect viral transcription by occupying the same catalytic region. Hemagglutinin binding was comparatively weaker than the sialic-acid reference, but the remaining hydrogen bonds and hydrophobic contacts still indicate site engagement that could help limit viral entry. Taken together, these interaction patterns suggest that anthocyanins may function as multi-site inhibitors, primarily through neuraminidase and PA endonuclease, with an additional, though less pronounced, effect on hemagglutinin. This provides a reasonable basis for considering them as natural lead candidates for further antiviral development.

3.5. ADMET and Drug-Likeness Screening

Physicochemical profiling (**Table 6**) showed that all anthocyanin glycosides exceeded Lipinski's limits, with molecular weights between 463.42 and 500.84 g/mol, high numbers of hydrogen bond donors (7–9) and acceptors (11-12), and low clogP values (–2.63 to –0.69). These features explain the predicted violations and suggest limited oral bioavailability.

ADMET predictions (**Table 7**) showed moderate aqueous solubility for all anthocyanin glycosides (–2.78 to –2.90 log mol/L) and variable predicted human intestinal absorption, with D3G showing the lowest absorption (17.03%) and P3G the highest (50.09%). These differences are consistent with the highly polar and glycosylated nature of the compounds. Distribution analysis indicated poor blood–brain barrier permeability (log BB < –1) and low CNS penetration, suggesting limited central nervous system exposure. None of the compounds were predicted to act as substrates or inhibitors of major CYP450 isoforms, indicating a low likelihood of metabolism-related drug–drug interactions. Predicted total clearance values were moderate (0.43–0.67 log ml/min/kg), and no compound was predicted to be a renal OCT2 substrate.

Toxicity evaluation, as part of the ADMET assessment, indicated a favorable safety profile. All compounds were predicted to be non-hepatotoxic and non-sensitizing to skin, with acceptable maximum tolerated dose values. In addition, pkCSM toxicity models include oral rat acute toxicity (LD_{50}-based) predictions, which estimate acute toxicity thresholds in animal models. Taken together, these results suggest low predicted acute and systemic toxicity for the studied anthocyanin glycosides.

Table 6. Molecular interactions of selected glycosides with target proteins based on docking studies, visualized in Discovery Studio

PDB ID	Ligands	H bond	Hypophobic/ Pi-cation/ Pi anion/ Pi-alkyl interaction
4MWW	C3G	GLY 349, ASN 348, GLU 279, LYS 294, GLU 246, ARG 153, TRP 180, GLU 120, ASN 296	ILE 224, ALA 248, ASP 152
	D3G	GLY 349, ARG 372, ASN 296, GLY 246, ARG 153, TRP 180, GLU 120, TYR 406, LYS 294	ILE 224, ALA 248, ASP 152
	Native	LYS 294, ARG 119, ARG 372, ARG 226, LYS 294	ILE 224, GLU 278, ASP 152
4BSD	C3G	ARG 121, VAL 177	LEU 144, TRP 142
	P3G	SER 134	LEU 144, TRP 142
	Native	GLY 216, GLY 219, SER 218, ARG 121, GLU 81, THR 125, ASN 123	HIS 174
6FS7	D3G	ILE 120, ILS 234, GLU 119, TYR 24, ILE 79, ARG 82,	ILU 106, GLU 80, ALA 87
	P3G	GLU 119, ALA 20, LYS 134, PRO 107	TYR 24, ALA 37, THR 38, LYS 34, HIS 41
	Native	LYS 34, LYS 134	THR 38, ALA 37, HIS 41, TYR 24

This open-access article is distributed under the terms of the Creative Commons Attribution Non Commercial 4.0 License (CC BY-NC 4.0).

Table 7. Predicted ADMET Properties of Selected glycosides Using pkCSM.

Compounds	Absorption				Distribution				Metabolism	Excretion		Toxicity		
	Water solubility (log mol/L)	Caco2 Permeability (log Papp in 10^{-6} cm/s)	HIA (% Absorbed)	Skin Permeability (log Kp)	VDss (human) (log L/kg)	Fraction unbound (human) (Fu)	BBB permeability (log BB)	CNS permeability (log PS)	CYP2D6 substrate CYP3A4 substrate CYP1A2 inhibitor CYP2C19 inhibitor CYP2C9 inhibitor	Total Clearance (log ml/min/kg)	Renal OCT2 substrate	Max. tolerated dose (human) (log mg/kg/day)	Hepatotoxicity	Skin Sensitisation
C3G	-2.90	0.26	29.92	-2.73	1.49	0.29	-1.37	-4.21	No; No; No; No; No	0.56	No	0.56	No	No
D3G	-2.86	-0.95	17.03	-2.73	1.14	0.31	-1.81	-4.85	No; No; No; No; No	0.59	No	0.51	No	No
P3G	-2.78	0.16	50.09	-2.73	0.84	0.14	-1.74	-3.94	No; No; No; No; No	0.62	No	0.56	No	No
M3G	-2.83	0.11	46.81	-2.73	0.93	1.15	-1.88	-4.3	No; No; No; No; No	0.67	No	0.43	No	No
Pt3G	-2.87	-0.97	42.39	-2.73	1.11	0.18	-1.94	-4.40	No; No; No; No; No	0.63	No	0.49	No	No

4. Conclusion

This study provides a computational assessment of five elderberry-derived anthocyanin glycosides against three influenza a viral proteins using molecular docking and predictive ADMET analyses. Among the evaluated compounds, cyanidin-3-glucoside showed the strongest predicted affinity toward neuraminidase, whereas delphinidin-3-glucoside and peonidin-3-glucoside demonstrated favorable predicted interactions with PA endonuclease. Docking validation supported the reliability of the docking protocol, and ADMET predictions indicated generally acceptable in silico pharmacokinetic and toxicity profiles, despite limited predicted oral bioavailability.

These findings represent preliminary computational evidence of potential multi-target interactions, not confirmation of antiviral activity. Therefore, biochemical enzyme inhibition assays, cell-based antiviral studies, pharmacokinetic investigations, and *in vivo* validation are required to determine the biological relevance of these predictions. Collectively, this work provides a computational basis for future experimental evaluation of elderberry anthocyanins as potential anti-influenza lead compounds.

Acknowledgment

The authors gratefully acknowledge the laboratory and institutional facilities that enabled the computational work in this study. We also thank the developers of SwissADME, AutoDock Vina, PyRx, Discovery Studio, and LigPlot+ for providing open-access and academic-licensing platforms essential for molecular modeling and interaction analysis.

Conflict of interest

The authors declare no conflicts of interest associated with this work.

Data availability

All data generated or analyzed during this study are included in the published article.

Authors Contributions

Samiran Sadhukhan: Conceptualization, methodology, investigation, data curation, formal analysis, visualization, and original draft preparation. Subarna Ganguli: Conceptualization, supervision, project administration, methodology, validation, critical review and editing, and intellectual guidance throughout the study. Both authors contributed to the scientific development of the manuscript and approved the final version.

Authors Orcid numbers:

Samiran Sadhukhan: 0009-0006-3089-9493
Subarna Ganguli: 0000-0002-7859-4721

Funding

The authors received no external funding for this research.

This open-access article is distributed under the terms of the Creative Commons Attribution Non Commercial 4.0 License (CC BY-NC 4.0).

Using artificial intelligence chatbots

Artificial intelligence tools were used to assist with language editing and manuscript preparation. The authors reviewed and revised the content and take full responsibility for the accuracy, integrity, and final version of the manuscript.

References

1. Iuliano AD, Roguski KM, Chang HH, Muscatello DJ, Palekar R, Tempia S, et al. Estimates of global seasonal influenza-associated respiratory mortality: a modelling study. The Lancet. 2018;391 (10127):1285–300.
2. Lampejo T. Influenza and antiviral resistance: an overview. Eur J Clin Microbiol Infect Dis. 2020 July;39 (7):1201–8.
3. Omoto S, Speranzini V, Hashimoto T, Noshi T, Yamaguchi H, Kawai M, et al. Characterization of influenza virus variants induced by treatment with the endonuclease inhibitor baloxavirmarboxil. Scientific reports. 2018;8(1):9633.
4. Chojnacka K, Skrzypczak D, Izydorczyk G, Mikula K, Szopa D, Witek-Krowiak A. Antiviral properties of polyphenols from plants. Foods. 2021;10(10):2277.
5. Torabian G, Valtchev P, Adil Q, Dehghani F. Anti-influenza activity of elderberry (Sambucus nigra). Journal of functional foods. 2019;54:353–60.
6. Dallakyan S, Olson AJ. Small-Molecule Library Screening by Docking with PyRx. In: Hempel JE, Williams CH, Hong CC, editors. Chemical Biology [Internet]. New York, NY: Springer New York; 2015 [cited 2025 Dec 4]. p. 243–50. (Methods in Molecular Biology; vol. 1263).
7. Wojciechowski M. Simplified AutoDock force field for hydrated binding sites. Journal of Molecular Graphics and Modelling. 2017;78: 74–80.
8. Trott O, Olson AJ. Software news and update AutoDock Vina: Improving the speed and accuracy of docking with a new scoring function. Effic. Optim. Multithreading. 2009;31: 455-61.
9. Shivanika C, Kumar D, Ragunathan V, Tiwari P, Sumitha A. Molecular docking, validation, dynamics simulations, and pharmacokinetic prediction of natural compounds against the SARS-CoV-2 main-protease. Journal of biomolecular structure & dynamics. 2020; 1.
10. Ayodele PF, Bamigbade A, Bamigbade OO, Adeniyi IA, Tachin ES, Seweje AJ, et al. Illustrated procedure to perform molecular docking using PyRx and Biovia discovery studio visualizer: a case study of 10kt with atropine. Progress in Drug Discovery & Biomedical Science [Internet]. 2023 [cited 2025 Dec 4];6(1).
11. C S, S. DK, Ragunathan V, Tiwari P, A. S, P BD. Molecular docking, validation, dynamics simulations, and pharmacokinetic prediction of natural compounds against the SARS-CoV-2 main-protease. J Biomol Struct Dyn. :1–27.
12. Daina A, Michielin O, Zoete V. SwissADME: a free web tool to evaluate pharmacokinetics, drug-likeness and medicinal chemistry friendliness of small molecules. Scientific reports. 2017;7(1):42717.
13. Azzam KA. SwissADME and pkCSM webservers predictors: An integrated online platform for accurate and comprehensive predictions for in silico ADME/T properties of artemisinin and its derivatives. KompleksnoeIspolzovanieMineralnogo Syra= Complex use of mineral resources. 2023;325 (2):14–21.
14. Liu Z, Zhao J, Li W, Wang X, Xu J, Xie J, et al. Molecular Docking of Potential Inhibitors for Influenza H7N9. Computational and Mathematical Methods in Medicine. 2015; 2015: 1–8.
15. Xiong X, Martin SR, Haire LF, Wharton SA, Daniels RS, Bennett MS, et al. Receptor binding by an H7N9 influenza virus from humans. Nature. 2013;499(7459):496–9.
16. Omoto S, Speranzini V, Hashimoto T, Noshi T, Yamaguchi H, Kawai M, et al. Characterization of influenza virus variants induced by treatment with the endonuclease inhibitor baloxavirmarboxil. Scientific reports. 2018;8(1):9633.
17. Ramírez D, Caballero J. Is It Reliable to Take the Molecular Docking Top Scoring Position as the Best Solution without Considering Available Structural Data? Molecules. 2018 May;23(5):1038.

This open-access article is distributed under the terms of the Creative Commons Attribution Non Commercial 4.0 License (CC BY-NC 4.0).